Journal of Inorganic and Organometallic Polymers and Materials
https://doi.org/10.1007/s10904-024-03331-w

RESEARCH

# Effect of Embedding $WO_3$NPs on the Structural, Morphological, Optical, and Dielectric Properties of PVA-CMC-PEG Polymeric Matrix Towards Optoelectronic and Energy Storage Applications

**Ihsan R. Ghanim[1] · Nisreen R. Aldulaimi[1] · Safa Ahmed Jabbar[2] · Fouad Sh. Hashim[2] · Karar Abdali[1] · Ehssan Al-Bermany[2] · Alaa Nihad Tuama[2]**

Received: 3 August 2024 / Accepted: 11 August 2024


**Abstract**
Pure and PVA-CMC-PEG films decorated with several low amounts of $WO_3$NPs doping were fabricated via the solution casting technique. The structural, morphological, optical, and dielectric properties of the as-prepared films were comprehensively investigated. FTIR analysis manifested that there was no change in the chemical structure of the polymer blend due to the decoration of $WO_3$NPs. FESEM images show that the control sample, F1, has a homogeneous texture, a smooth surface, and no cracks, and the infused $WO_3$NPs were finely distributed as grids and wrinkled-like shapes on the surface of the matrix. The optical results revealed an immense enhancement in the absorbance, from 33 to 98%. The allowed and forbidden indirect band gaps of the F1 sample (4.35 eV, 4.20 eV) dropped to (3.60 eV, 3.25 eV) in the F4 sample. The DC electrical conductivity of the nanocomposite films was notably increased from $1.93\times10^{-8}$ $\Omega.cm^{-1}$ to $1.14\times10^{-5}$ $\Omega.cm^{-1}$ with an increase in the amount of $WO_3$NPs at 90 °C. The DC results also indicated that all films have a single activation energy, whose values decreased from 2.2580 to 1.4007 eV. The effect of $WO_3$NPs on the AC conductivity and dielectric constants was studied, where the dielectric constant of the nanocomposite films was higher than that of the host matrix with a reduced dielectric loss. Ultimately, these films are promising candidates for optoelectronic and energy storage applications.

**Keywords** PVA-CMC-PEG · $WO_3$ · Optical properties · Dielectric properties · Energy storage

## 1 Introduction

Polymer-freestanding nanocomposites (PFNCs) are an important subject in the development and production of materials, particularly polymer nanomaterials [1]. It is well recognized that the most significant factors resulting from the interaction of filler nanoparticles with polymers are PFNCs that improve their properties [2].

Poly (vinyl alcohol) (PVA) has a relatively simple chemical structure. There are commercial PVA modifiers with high grades of hydrolysis. The grades of hydrolysis, or the number of acetate collections in the polymer, have an impact on its biochemical properties, solubility, and crystallization [3]. It is distinguished from other polymers by good properties such as lightweight, low-cost, wear resistance, strength, high optical quality, and environmentally friendly [4]. Carboxymethyl cellulose (CMC), generally used as the sodium salt Na-CMC, is one of the most widely used polyelectrolyte cellulose derivatives. Na-CMC has vast applications in the food, pharmaceutical, personal care/cosmetic, paper, optoelectronics, and other industries. CMC, like many other water-soluble substances, may be salted out of solution with alkali metal salts. However, because of the very hydrophilic nature of the polymer, CMC is much more tolerant of many types and concentrations of salt than other hydrocolloids such as carrageenan, alginates, or pectin, which are highly sensitive to particular salts, e.g., calcium. CMC exhibits several interesting and useful rheological properties upon reaching complete dissolution. CMC is a biodegradable,

✉ Karar Abdali
aaazezphys@gmail.com

[1] Iraq Ministry of Education, Baghdad, Iraq

[2] Department of Physics, College of Education for Pure Science, University of Babylon, Babylon, Iraq

Published online: 28 August 2024

cost-effective, water-soluble polymer with semicrystalline natures that is non-toxic and capable of producing high-quality films. CMC shows many advantageous characteristics, including suspension, filming, binding, emulsificatin, water retention, and thickening [5].

Polyethylene glycol (PEG) is a synthetic biodegradable polymer and applied to several applications like food industries, biomedical, optoelectronics, sunscreens, sensors, shielding, etc. [6].

Transition metal oxides are an important class of semiconductors and have been extensively studied. Because of their distinctive properties for potential applications such as solar cells, electronics, catalysis, optical light, and antibacterial [7]. Among the transition metal oxides, tungsten trioxide nanoparticles ($WO_3$NPs) are a p-type semiconductor and yellow powder material with an energy gap between 2.5 eV and 3.0 eV and are found in different crystal structure phases depending on temperatures. $WO_3$NPs have various applications in flexible and transparent electronics, such as displays, sensors, and integrated circuits [8, 9].

There are many research papers reporting the impact of $WO_3$NPs on the physical performance of the polymer matrix [10–13]. By comparing our results with that obtained by literatures we found that the present study give superior findings.

The PFNCs of polymers and transition metals have a great advantage as they hold the ability for simultaneous enhancement of the dielectric constant, leading to notable boosts in energy storage applications.

To objectively evaluate the novelty of our study, a comparative literature scan was carried out to show similar research studies concerning the use of PVA-CMC-PEG/WO3NP PFNC films or comparable methodologies in optoelectronic and energy storage applications.

This study aims to explore the influences of varying $WO_3$NPs wt% on the morphological, structural, optical, DC, and AC electrical properties of PVA-CMC-PEG polymeric matrix to be suitable for different optoelectronic device and energy storage applications.

## 2 Materials and Methods

### 2.1 Materials

Highly pure $WO_3$NPs (> 99.8%, 30 nm) were purchased from Sigma-Aldrich; PVA (99.8%, 185,000 g/mol) was purchased from Himedia, India; and CMC (99.9%, 700,000 g/mol) was purchased from Glentham Life Sciences Ltd., United Kingdom; PEG (99.7% 6000 g/mol) from Sigma-Aldrich. Ultra-pure water (UPW) was used as a solvent for all experiments.

**Table 1** The ratios of PVA-CMC-PEG and WO3NPs

| Sample ID | PVA-CMC-PEG ratio | WO3NPs wt% |
|---|---|---|
| F1 | 90% – 5% – 5% | 0 |
| F2 | | 2 |
| F3 | | 4 |
| F4 | | 6 |

### 2.2 Preparation of Nanocomposite Films

Briefly, 0.9 g of PVA in 30 mL UPW was dissolved for 1 h using a magnetic stirrer, and then the temperature was increased to 50 °C and continued for another period. After that, 0.05 g of CMC and 0.05 g of PEG were added to synthesize the PVA-CMC-PEG polymer matrix. The resulting solution was poured into a plastic Petri dish and kept in the air at RT for 120 h to dry. The same method was followed in the preparation of PBNC films based on (2, 4, and 6 wt%) of $WO_3$NPs. The ratios of PVA-CMC-PEG and WO3NPs were illustrated in Table 1.The thicknesses of the prepared films were about $80 \pm 3$ µm, as measured by the digital Vernier Caliper. The samples were listed as F1, F2, F3, and F4 respectively.

### 2.3 Descriptions

The samples' functional groups were ascertained using Fourier transform infrared spectroscopy (FTIR, Bruker, vertex-70 spectrometer, German) in the wavenumber region of 4000–500 $cm^{-1}$; the surface morphologies were analyzed using field emission scanning electron microscopy (FESEM, MIRA3 TESCAN); a Shimadzu (UV-1800 A) spectrophotometer was used to measure film transmission curves in the wavelength range of 200–1100 nm; the dielectric characteristics were studied in the frequency range of $f = 10^2$ to $5 \times 10^6$ Hz by LCR meter (HIOKI 3532-50 LCR HI TESTER); the thicknesses of the prepared films were measured by the digital Vernier Caliper.

## 3 Results and Discussion

### 3.1 FESEM Analysis

The surface morphologies of F1 (reference sample) and their nanocomposite films with $WO_3$NPs (F2-F4) were comprehensively investigated using FESEM, as shown in Fig. 1. It can be observed from Fig. 1-a that the F1 film (control sample) has a homogeneous texture, a smooth surface, and no cracks. However, the infusing of different amounts (2%, 4%, and 6%) of $WO_3$NPs into PVA-CMC-PEG (Fig. 1, b–d) shows a fine distribution of the $WO_3$NPs within the reference sample by forming seamless spider web-like or

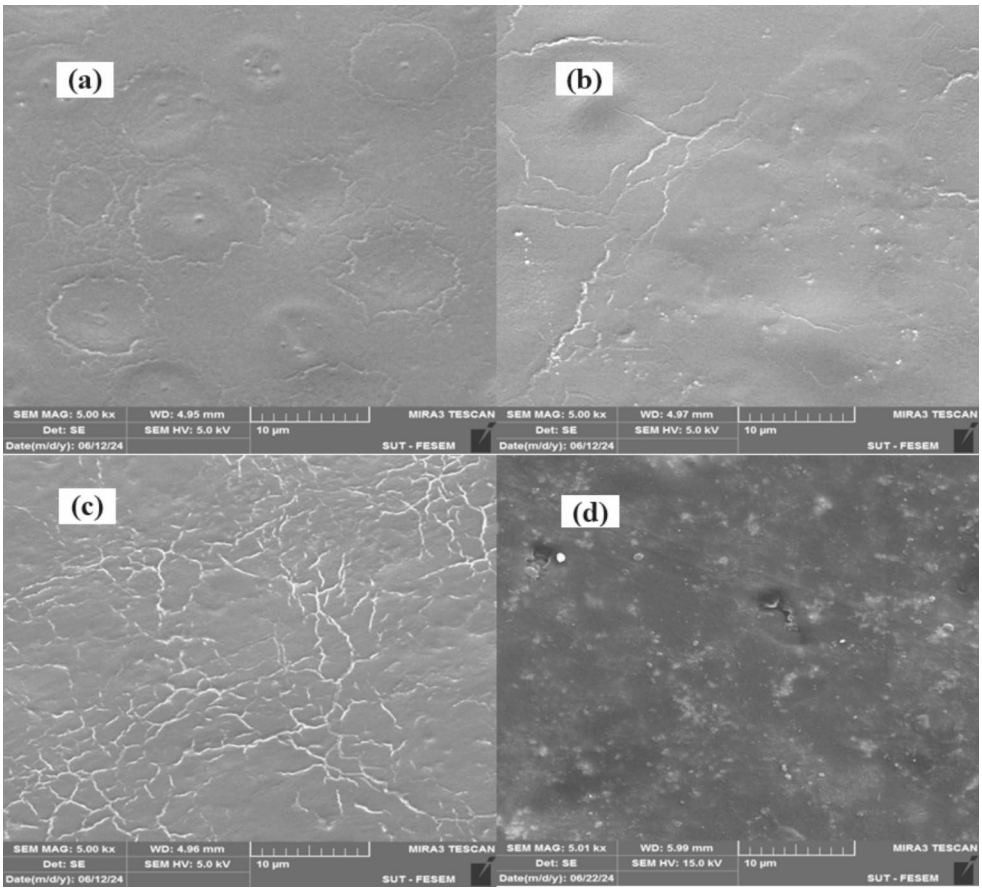


**Fig. 1** FESEM microstructure images of a- F1, b- F2, c- F3, and d- F4 samples

grid-like shapes on the surface of matrix (Figs. b and c) that convert to a simple wrinkled-like shape in the F4 sample (Fig. 1, d). Remarkably, the surface roughness of the matrix surface was raised by increasing the amount of $WO_3$NPs.

### 3.2 FTIR Investigation

The FTIR spectra of the PVA-CMC-PEG polymeric blend and their PFNCs with different weights of $WO_3$NPs are conclusively shown in Fig. 2. The basic composition structure of PVA polymer is $(C_2H_4O)n$ [10], and that of CMC and PEG polymer are $[C_6H_{10}O_5]_n$ [11]. The broad peak observed at approximately 3282.48 $cm^{-1}$ is hydroxyl-OH group stretching vibration, and the peak that occurs at 2891.50 $cm^{-1}$ indicates a methyl C-$H_3$ asymmetrical band of stretching [12]. The peak observed at 1728.08 $cm^{-1}$ can be ascribed to the carbonyl group C = O stretching bond [13]. Meanwhile, the functional groups at 1342.38 $cm^{-1}$, 1240.53 $cm^{-1}$, and 1111.71 $cm^{-1}$ can be attributed to the amide group and OH group bending vibrations of the PFNCs and to the presence of C-O stretching vibrations of PVA, CMC, and PEG, respectively [14, 15]. Moreover, the C-C stretching vibrational mode of the PVA molecules is shown by the absorption peak that appears at 955.06 $cm^{-1}$, and the peak at 841.69 $cm^{-1}$ corresponding to peroxide C-O-O– stretching [16, 17]. FTIR results indicate that there is no shift of the functional groups, which indicates that the hydrogen bonds were formed through the physical interaction between the absorption bands of the polymer matrix and their PBNC films.

### 3.3 The Optical Properties

The UV-visible absorbance spectra (A) of the PVA-CMC-PEG blend polymer and their PFNCs with different loadings of $WO_3$NPs are shown in Fig. 3. It is evident that in the VIS and NIR, the absorbance curves show a tendency towards saturation, and an enhancement in its absorbance values is noted from 33 to 98% for the F4 sample compared to the F1 reference sample in the UV region. The UV spectra's high-intensity absorption edge was at about 240 nm for the F1 control sample. The noticeable variance in this absorption edge height among F2, F3, and F4 specimens is attributed to the disorder reasoned by WO3NPs filled the blend matrix [18]. This result occurs due to the ability of electrons to absorb electromagnetic energy (EM) interacting with atoms and move to higher energy levels [19].

The Swanepoel relationship (Eq. 1) was used to compute the absorption coefficient α [20]:

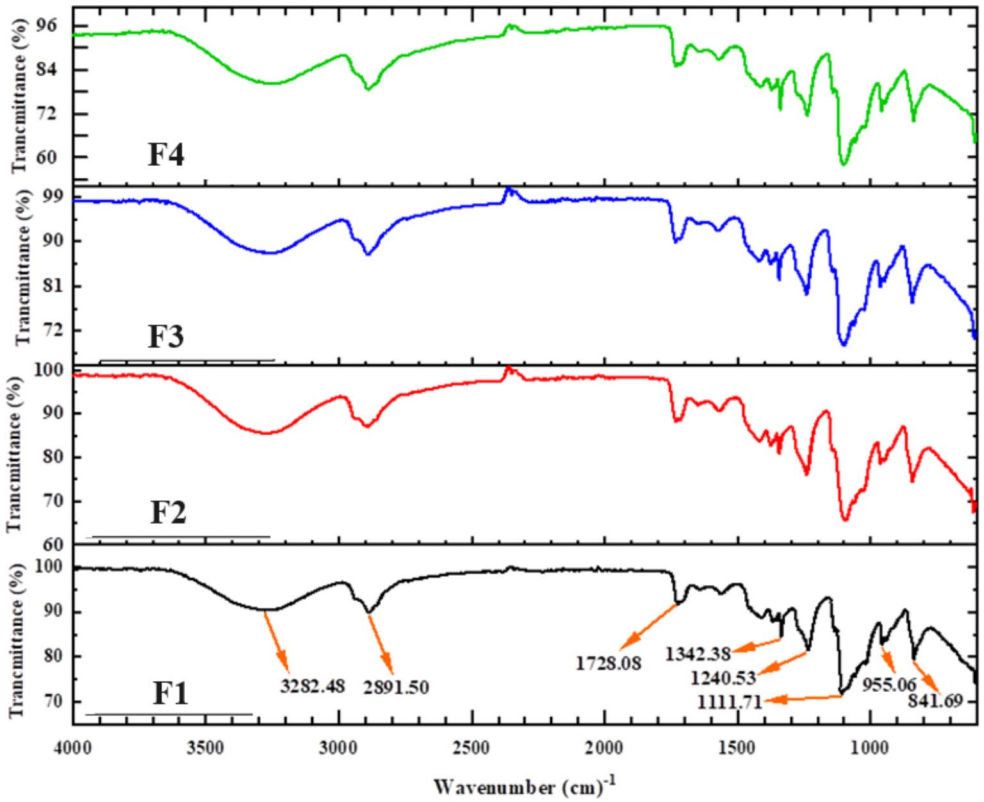


**Fig. 2** FTIR spectra of a- F1, b- F2, c- F3, and d- F4 samples

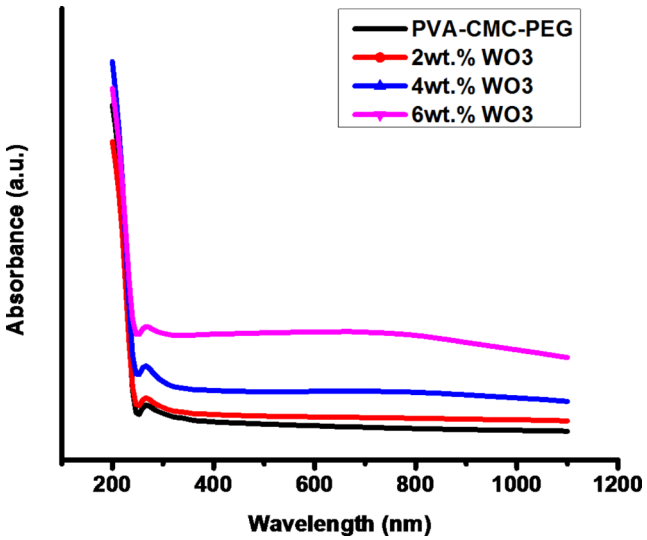


**Fig. 3** UV-visible absorbance spectra of blended polymer and its PFNCs

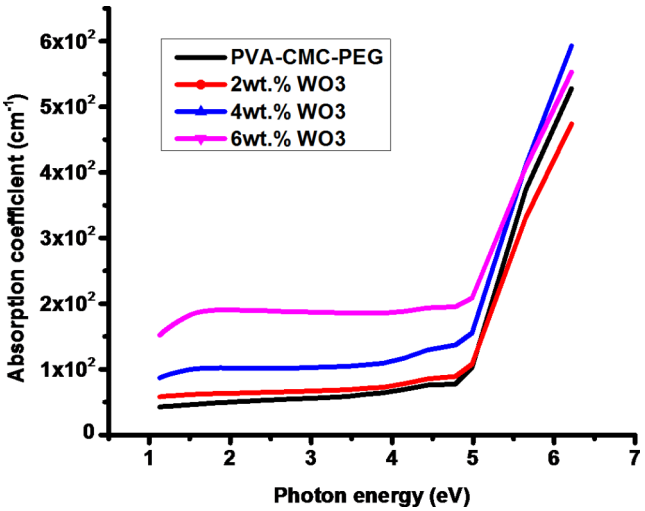


**Fig. 4** Absorption coefficient spectra of blended polymer and its PFNCs

$$\alpha = 2.303 \left(\frac{A}{t}\right) \quad (1)$$

Where t is the thickness of the film, α values can be used to distinguish between direct and indirect types of electronic transitions. If $\alpha > 10^4$ $cm^{-1}$, electrons should be transferred directly, while if $\alpha < 10^4$ $cm^{-1}$, they should be transmitted indirectly. In the current work, the α values were lower than $10^4$ $cm^{-1}$, which refers to the appearance of indirect electronic transitions as shown in Fig. 4.

Using the thickness-dependent Tauc's relation (Eq. 2), the optical energy gap of the produced films was computed from the absorbance data [20].

$$(\alpha\, h\upsilon)^m = B(h\upsilon - E_g^{opt} \pm E_{ph}) \quad (2)$$

Where B is the parameter for band tailing, and *m* defines the type of optical transition for the materials under investigation (m = 1/2 for allowed indirect transitions and m = 1/3 for forbidden indirect transitions). The values obtained from the plot of $(\alpha h\nu)^{1/2}$ and $(\alpha h\nu)^{1/3}$ against photon energy (hν) shown in Figs. 5 and 6 were included in Table 2.

The indirect for allowed and forbidden electronic transitions of the F1 sample and their PBNC films with several amounts of $WO_3$NPs was calculated by projecting the linear portion of the curve to the photon energy axis. It can be observed that both allowed and forbidden indirect decreased from 4.35 to 3.60 eV and from 4.20 to 3.25 eV, respectively, with the decoration of $WO_3$NPs. The change in the crystallinity of the films and oxygen ion vacancies may cause a reduction in the optical energy gap; these positively charged vacancies may capture some free electrons and act as donor centers, leading to a reduction in the optical energy gap. From another point of view, the formation of imperfections and disarrays in the materials, which are close to the conduction band, may explain why the optical energy gap has reduced [21, 22].

The complex dielectric function (ε) is a measure of a material's ability to reduce the speed of light within it based on its energy storage. The real part represents the material's capacity to reduce light speed, while the imaginary part illustrates how materials absorb energy from the electric field due to dipole motion. These values can be calculated using Eqs. 3 and 4 [23]:

$$\epsilon_{\,r} = n^2 - k_\circ^2 \tag{3}$$

$$\epsilon_{\,i} = 2nk_\circ \tag{4}$$

where $\epsilon_{\,r}$, $\epsilon_{\,i}$, n, and $k_\circ$ are the dielectric constants, dielectric loss, the refractive index, and the extinction coefficient, respectively. The variation of the dielectric constant as a function of wavelength is seen in Figs. 7 and 8. From the findings, the F1 sample dielectric constant increases for both the real and imaginary components at shorter wavelengths. The real and imaginary values of the PBNC films show a noticeable higher value in comparison with F1 polymeric blend sample at all wavelengths. The enhancement of the dielectric constant is influenced by the interfacial polarization between the $WO_3$NPs filler and matrix [24–27].

### 3.4 D.C Electrical Properties

The behavior of the electrical conductivity of the direct current ($\sigma_{dc}$) in the various temperature (T) ranges from 30 °C to 90 °C for the F1 polymer blend sample and their PBNC films was studied, as illustrated in Fig. 9. The increase in $\sigma_{dc}$ after the incorporation of $WO_3$NPs at all temperatures could be attributed to the formation of connected networks in the polymeric matrix. On the other hand, as we know, the current nano-fillers are semiconductor materials, and mixing them with PVA-CMC-PEG may lead to the formation of sub-energy levels inside the band gap, which act as

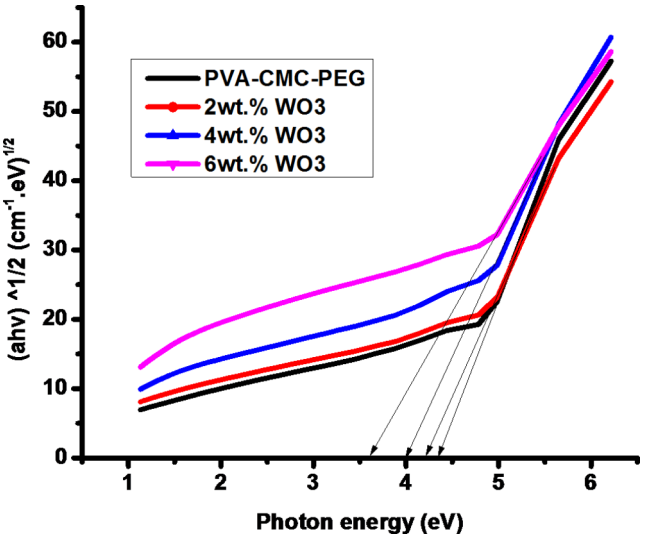


**Fig. 5** Variation $E_{g\,indir}^{opt}$ for allowed transition of blended polymer and its PFNCs

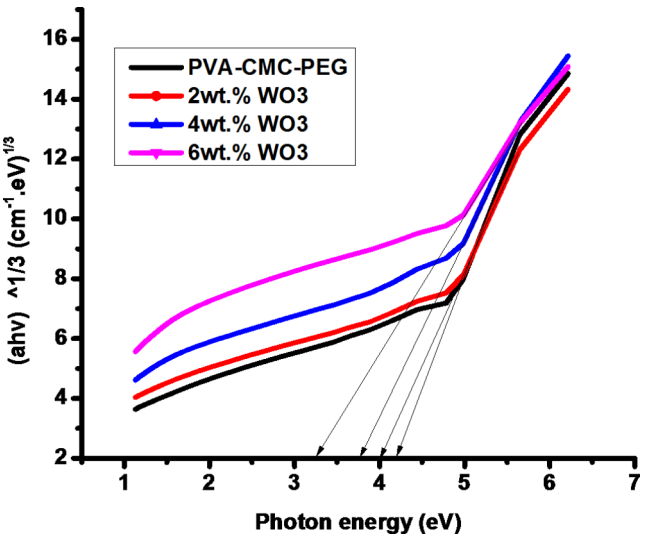


**Fig. 6** Variation $E_{g\,indir}^{opt}$ for forbidden transition of blended polymer and its PFNCs

**Table 2** $E_{g\,indir}^{opt}$ values for the allowed and forbidden indirect transition of blended polymer and its PFNCs

| Sample ID | $E_{g\,indir}^{opt}$ allowed | $E_{g\,indir}^{opt}$ forbidden |
|---|---|---|
| F1 | 4.35 | 4.20 |
| F2 | 4.25 | 4.00 |
| F3 | 4.00 | 3.80 |
| F4 | 3.60 | 3.25 |

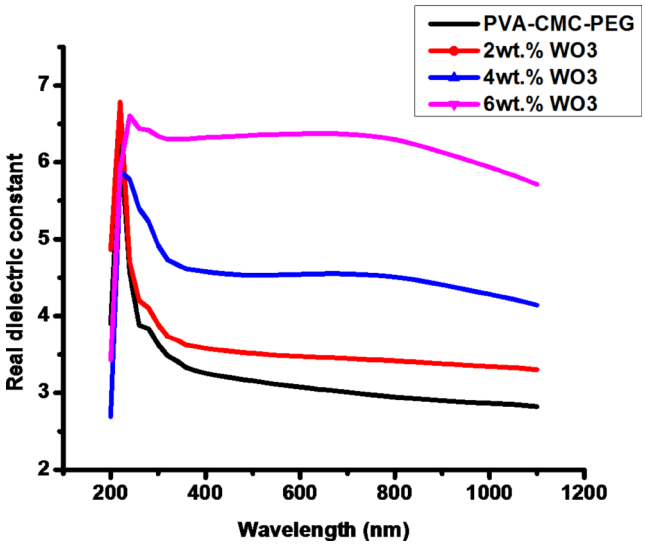


**Fig. 7** Real part of dielectric constant spectra of blended polymer and its PFNCs

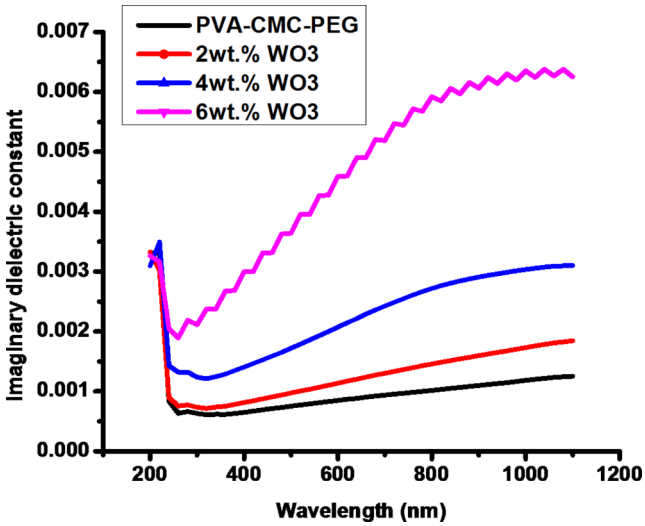


**Fig. 8** Imaginary part of dielectric constant spectra of blended polymer and its PFNCs

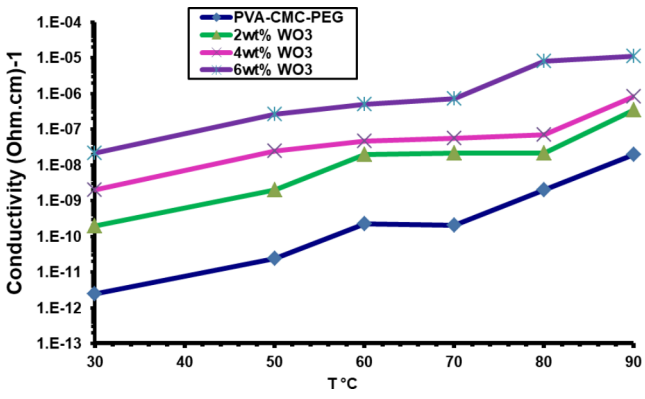


**Fig. 9** The dependence of conductivity ($\sigma_{dc}$) of blended polymer on temperature and nano-fillers concentration

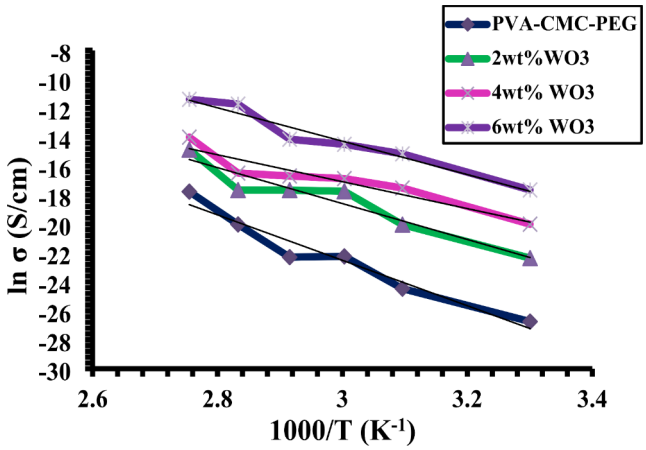


**Fig. 10** ln $_{\sigma}$ versus $10^3$/T of blended polymer and its PFNCs

**Table 3** The experimental results of the $E_{ac}$ values

| Sample | $E_{ac}$ (eV) |
|---|---|
| F1 | 2.2580 |
| F2 | 1.8863 |
| F3 | 1.5215 |
| F4 | 1.4007 |

traps for charge carriers that move by hopping among these levels, resulting in an increase in $\sigma_{dc}$ [28]. The maximum $\sigma_{dc}$ values that appear at 90 °C are $1.93\times10^{-8}$, $3.51\times10^{-7}$, $8.33\times10^{-7}$, and $1.14\times10^{-5}$ Ω.cm$^{-1}$ for F1, F2, F3, and F4 samples, respectively. Similar behavior was reported by [29].

Figure 10 shows the variation of lnσ versus $10^3$/T measured at temperature range between 303 K and 363 K for polymeric blend and its PFNCs. To calculate the activation energy ($E_{ac}$), Arrhenius equation was used [30]:

$$\sigma = \sigma_o \exp(-E_{ac}/K_B T) \quad (5)$$

where $\sigma_o$ is the conductivity at RT, $E_{ac}$ is the activation energy, $K_B$ is Boltzmann constant, and T is temperature.

The calculated results of $E_{ac}$ values range from 2.2580 eV to 1.4007 eV, as displayed in Table 3. The high value of $E_{ac}$ for the F1 polymeric blend is attributed to the existence of free ions in the polymers, which move by the hopping process. The decrease in $E_{ac}$ is related to an increase in local energy levels in the energy gap, which act as traps for charge carriers and play an important role in charge transport [31].

## 3.5 AC Electrical Properties

Dielectric constant (ε′), dielectric loss (ε”), and AC electrical conductivity ($\sigma_{AC}$) for polymer blend and their nanocomposites with WO3NPs films were studied at RT over the

frequency range $10^2$ -$5\times10^6$ Hz, and computed using the following formulas [32, 33]:

$$\varepsilon' = C_P/C_o \tag{6}$$

$$\varepsilon'' = \varepsilon' D \tag{7}$$

$$\sigma_{A.C} = \omega\,\varepsilon''\varepsilon_0 \tag{8}$$

The $C_o$ is usually used to denote a vacuum capacitor, whereas the term $C_p$ is generally used to describe capacitance. The variable "displacement" (D) is utilized in this context, and ω represents the angular frequency.

The dielectric constant, dielectric loss, and AC electrical conductivity for the F1 polymer blend and their PBNC films with different loading ratios of $WO_3$NPs were systemically studied at RT over the frequency range of $10^2 - 5\times10^6$ Hz. Figure 11 shows the dependence of the dielectric constant on frequency. Decreasing the dielectric constant with increasing frequency may be attributed to the tendencies of the dipole in the samples for orienting themselves in the directions of the applied electrical field and decreasing space charge polarization [32, 33]. The maximum dielectric constants at 100 Hz are 0.518, 6.333, 10.320, and 39.346 for the F1, F2, F3, and F4 samples, respectively. These values also revealed the ability of these films to store energy from the applied electric field.

The dielectric loss measures the lost electrical energy in the sample from the applied field, which is transformed into thermal energy in the sample. The dependence of dielectric loss on electric field frequency and $WO_3$NPs dopant at RT is shown in Fig. 12. The maximum dielectric losses are 0.632, 14.567, 30.961, and 173.124 for the F1 polymer blend and its PFNCs with different weights of WO3NPs, respectively. The decrease in dielectric loss values with increasing frequency of applied electric field is attributed to a decrease in the space charge polarization contribution [34].

The dependence of AC electrical conductivity on frequency at RT is shown in Fig. 13. The AC conductivity increases considerably with the increase in frequency for all samples, which is attributed to the space charge polarization along the frequency used and to the motion of charge carriers by the hopping process. Also, the conductivity increases with the increasing weight of $WO_3$NPs. This behavior is due to the effect of the space charge as a result of the increase in charge carriers due to the regular distribution in the polymeric matrix. Then, if electrical polarization had the highest effect in one specimen, it would also have the most effect in all other specimens. Considering this, electrical conductivity and polarization are given a high value for the dielectric constant. The F4 specimen gave the highest electrical enhancement, and therefore this sample is extremely

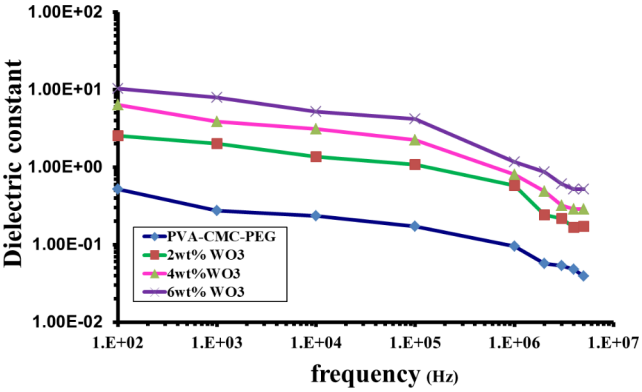


**Fig. 11** The dependence of dielectric constant of the prepared films on frequency and dopant amounts

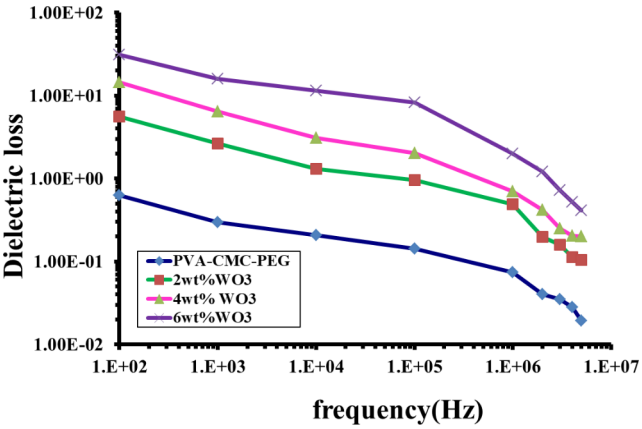


**Fig. 12** The dependence of dielectric loss on frequency and dopant amounts

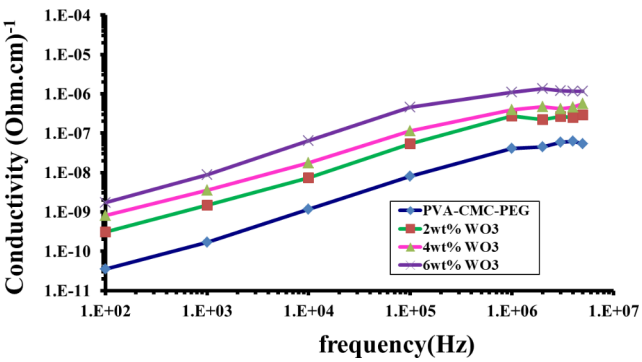


**Fig. 13** The dependence of AC electrical conductivity on frequency and dopant amounts

promising for the development of energy storage devices [35–37].

## 4 Conclusions

Novel PVA-CMC-PEG/$WO_3$NPs nanocomposite films, based on PVA-CMC-PEG as a matrix material and $WO_3$NPs as a dopant material, were successfully created using the solution casting procedure. The FTIR confirmed that there is no change in the chemical structures between the polymer blend and the additives. FESEM microstructures illustrate that the matrix sample, F1, has a homogeneous texture, a smooth surface, and no cracks, and the embedding $WO_3$NPs were finely distributed as grids and wrinkled-like shapes on the surface of the matrix. The optical results of nanocomposite film revealed an immense enhancement from 33 to 98% in its absorbance compared to matrix in the UV region. The allowed and forbidden indirect band gaps of blend polymers dropped upon infusing $WO_3$NPs. The DC electrical conductivity of the polymeric system increased after the addition of $WO_3$NPs at all temperatures, and the measurements indicated that all films have a single activation energy, whose values decrease as a function of increasing temperature. The AC electrical properties showed that the dielectric constant and dielectric loss for all samples decreased with the increase in electric field frequency, but the AC conductivity of the nanocomposites increased with the loading of WO3NPs. The effect of WO3NPs on the AC conductivity and dielectric constants was studied, where the dielectric constant of the nanocomposite films was higher than that of the host matrix with a reduced dielectric loss. Ultimately, the developed ternary nanocomposite films can find potential applications in the optoelectronic and energy storage fields.

**Acknowledgements** Thanks for university of Babylon-college of education for pure science.

**Author Contributions** "All authors contributed to performing all the experiments, data analysis, and writing the first draft paper. IR and NR contributed to the FTIR and measured the optical constants, FS analyzed the optical properties. whereas EB and AN did the SEM and the introduction section of the manuscript. KA wrote and polished the final version of the paper, participated in the conception of the experiment, and improved the quality of the manuscript through SEM images. SA did the AC and DC testing. All authors read and approved the final manuscript."

**Funding** No funds were received.

**Data Availability** No datasets were generated or analysed during the current study.

## Declarations

**Ethical Approval** Not applicable.

**Competing Interests** The authors declare no competing interests.

## References

1. M.A. Salam, F.H. Alsultany, E. Al–Bermany, M.M. Sabri, K. Abdali, N.M. Ahmed, Impact of graphene oxide nanosheets and polymethyl methacrylate on nano/hybrid–based restoration dental filler composites: ultrasound behavior and antibacterial activity. J. Ultrasound. (2024). https://doi.org/10.1007/s40477-023-00855-8
2. F.S. Hashim, S.H. Idres, A.N. Tuama et al., Microstructure, Optical, and Antibacterial features of PVP/Cu2O Electrospun Nanofibers for Optoelectronics and Biological purposes. J. Inorg. Organomet. Polym. (2024). https://doi.org/10.1007/s10904-024-03201-5
3. N.A.P. Christie, M. Hassan, Structure and applications of poly(vinyl alcohol) hydrogels produced by conventional crosslinking or by freezing/thawing methods. Adv. Polym. Sci. **153**, 37–65 (2000). https://doi.org/10.1007/3-540-46414-x_2
4. A.Y. Yassin, A.M. Abdelghany, R.S. Salama et al., Structural, optical and antibacterial activity studies on CMC/PVA Blend filled with three different types of Green synthesized ZnO nanoparticles. J. Inorg. Organomet. Polym. **33**, 1855–1867 (2023). https://doi.org/10.1007/s10904-023-02622-y
5. A.Y. Yassin, E.M. Abdelrazek, A.M. Abdelghany, E.M. Abdallah, Incorporated Au/Se nanoparticles into HPMC/CMC blend for enhancing structural, optical and morphological properties: hybrid nanocomposites for optoelectronic applications, Optical materials, **154**, 2024. https://doi.org/10.1016/j.optmat.2024.115721
6. A.M. El-naggar, Z.K. Heiba, A.M. Kamal et al., Linear and nonlinear optical characteristics of PVA/CMC/PEG blended polymer loaded with ZnS formed at different temperatures. J. Mater. Sci: Mater. Electron. **34**, 114 (2023). https://doi.org/10.1007/s10854-022-09460-7
7. A.N. Tuama, E. Al-Bermany, R.S. Alnayli, Khalid Haneen Abass, Karar Abdali & Muhammad Hasnain Jameel, a critical review of the evaluation of Sio2-Incorporated Tio2 nanocomposite for photocatalytic activity. Silicon. (2024). https://doi.org/10.1007/s12633-024-02870-8
8. E.T. Salim, J.A. Saimon, M.S. Muhsin et al., Synthesis of $WO_3$ NPs by pulsed laser ablation: Effect of laser wavelength. J. Mater. Sci: Mater. Electron. **35**, 533 (2024). https://doi.org/10.1007/s10854-024-12249-5
9. M.S. Muhsin, E.T. Salim, J.A. Saimon, Structural, Morphological and optical properties of tungsten trioxide nanoparticle synthesis by pulsed laser ablation in water: effect of laser fluence. J. Opt. **53**, 2339–2354 (2024). https://doi.org/10.1007/s12596-023-01368-7
10. S. Yazan Badour, S. Danto, S. Albakour, N. Mornet, Penin et al., Low-cost WO3 nanoparticles / PVA smart photochromic glass windows for sustainable building energy savings, Solar Energy Materials and Solar Cells, 255, 112291, 202310.1016/j.solmat.2023.112291
11. M.A. Morsi, I. Ahlam, F. Al-Sulami, H. Mohammad, M.O. Al Sulami, M.A. Farea, A.A. Alqarni, A. Alhazime, Rajeh, Preparation, structural characterization, optical, photoluminescence, AC electrical conductivity and broadband dielectric properties of WO3 reinforced PEG/CS blend for futuristic optoelectronic and energy storage devices. Results Phys. **59** (2024). https://doi.org/10.1016/j.rinp.2024.107582

12. N.B. Rithin Kumar, V. Crasta, B.M. Praveen, Dielectric and electric conductivity studies of PVA (Mowiol 10–98) doped with MWCNTs and WO3 nanocomposites films. Mater. Res. Express. (2016). https://doi.org/10.1088/2053-1591/3/5/055012
13. K. Suzuko Yamazaki, Isoyama, Kinetic studies of WO3-Based photochromism in polyvinyl Alcohol Film. ACS Publications. **29** (2023). https://doi.org/10.1021/acs.langmuir.3c01227
14. F.S. Hashim, S.A. Jabbar, E. Al-Bermany et al., Effect of Inclusion ZnO-Co3O4 Nanoparticles on the Microstructural and Optical Properties of PVA-PEG Polymeric Blend for Biomedical, UV Shielding, and Nuclear Radiation Shielding Applications. Plasmonics, 2024 (2024). https://doi.org/10.1007/s11468-024-02379-1
15. A.M. Kadim, K.H. Abass, K. Abdali et al., Effect of loading corn starch nanoparticles on the morphological, optical, and dielectric behaviors of pva/pmma/paam polymer blend for optoelectronic and antibacterial applications. Nano Biomed. Eng. **16**(1), 119–127 (2024). https://doi.org/10.26599/NBE.2024.9290049
16. Karar Abdali, Structural, optical, electrical properties, and relative humidity sensor application of PVA/Dextrin polymeric blend loaded with silicon dioxide nanoparticles. J. Mater. Sci.: Mater. Electron. (2022). https://doi.org/10.1007/s10854-022-08676-x
17. K. Abdali, E. Al-Bermany, K.H. Abass, Impact the silver nanoparticles on properties of new fabricated polyvinyl alcohol-polyacrylamide- polyacrylic acid nanocomposites films for optoelectronics and radiation pollution applications. J. Polym. Res. **30**, 138 (2023). https://doi.org/10.1007/s10965-023-03514-y
18. A.A.F. Abodood, K. Abdali, A.O. Mousa Al-Ogaili, Effect of molar concentration and solvent type on linear and NLO properties of aurintricarboxylic (ATA) organic dye for image sensor and optical limiter applications. Int. J. Nanosci. (2023). https://doi.org/10.1142/S0219581X2350014X
19. A.Y. Yassin, Synthesized polymeric nanocomposites with enhanced optical and electrical properties based on gold nanoparticles for optoelectronic applications. J. Mater. Sci: Mater. Electron. **34**, 46 (2023). https://doi.org/10.1007/s10854-022-09402-3
20. J. Tauc, A. Menth, D.L. Wood, Optical and magnetic investigations of the localized states in semiconducting glasses. Phys. Rev. Lett. **25**(11), 749 (1970)
21. K. Abdali, Novel flexible Glass Composite Film for Stretchable devices Applications. Silicon. (2023). https://doi.org/10.1007/s12633-023-02414-6
22. M.A. Saadiah, D. Zhang, Y. Nagao, S.K. Muzakir, A.S. Samsudin, Reducing crystallinity on thin film based CMC/PVA hybrid polymer for application as a host in polymer electrolytes. J. Non Crystalline Solids. **511**, 201–211 (2019). https://doi.org/10.1016/j.jnoncrysol.2018.11.032
23. A. Karar, F. Lamis, A. Alhak, O. Abdulazeez, Enhancing some physical properties of Cosmetic Face Powders. J. Global Pharma Technol. **10**, 75–78 (2018)
24. K.H. Karar Abdali, E. Abass, Al-Bermany et al., Morphological, optical, ElectricalCharacterizations and Anti-escherichia Coli Bacterial Efficiency (AECBE) of PVA/PAAm/PEO Polymer Blend Doped with Silver NPs. Nano Biomed. (2022). https://doi.org/10.5101/nbe.v14i2.p114-122
25. K.H. Alharbi, W. Alharbi, M.A. El-Morsy, M.O. Farea, A.A. Menazea, Optical, Thermal, and Electrical characterization of polyvinyl Pyrrolidone/Carboxymethyl cellulose blend scattered by Tungsten-Trioxide Nanoparticles. Polymers. **15**, 1223 (2023). https://doi.org/10.3390/polym15051223
26. H.H. Jassim, F.S. Hashim, Synthesis of (PVA/PEG: ZnO and Co3O4) nanocomposites: Characterization and antibacterial studies, in *AIP Conference Proceedings*, 2022, vol. 2398, no. 1
27. S.A. Jabbar, S.M. Khalil, A.R. Abdulridha et al., Dielectric, AC Conductivity, and optical characterizations of (PVA-PEG) Doped SrO Hybrid nanocomposites. Key Eng. Mater. **936**, 83–92 (2022). https://doi.org/10.4028/p-41a757
28. R. Divya, M. Meena, C.K. Mahadevan, C.M. Padma, Formation and Properties of ZnO Nanoparticle dispersed PVA films. Int. J. Eng. Res. Technol. **3**, 722–727 (2014)
29. H.H. Jassim, F.S. Hashim, Synthesis of (Pva/peg: Zno and co3o4) nanocomposites: Characterization and gamma ray studies, NeuroQuantology, 19, 4, pp. 47–56, 2021, https://doi.org/10.14704/nq.2021.19.4.NQ21036
30. S.A. Arrhenius, Über die Dissociationswärme und den Einfluß Der Temperatur auf den Dissociationsgrad Der Elektrolyte. Z. Phys. Chem., **4**, pp. 96–116, 1889. https://doi.org/10.1515/zpch-1889-0408. S2CID 202553486
31. A.M. El-naggar, L.A. Alsulaymani, M.B. Mohamed et al., Structural, DC Conductivity and Dielectric characteristics of PVA/CMC/PPy/Melanin Blended Polymer Composites for Energy Storage Applications. J. Inorg. Organomet. Polym. (2024). https://doi.org/10.1007/s10904-024-03184-3
32. B.H. Karar Abdali, E. Rabee, Al-Bermany, Effect of doping Sb2O3NPs on morphological, mechanical, and dielectric properties of PVA/PVP blend film for electromechanical applications. Nano. (2023). https://doi.org/10.1142/S179329202350011X
33. K. Abdali, E. Al-Bermany, A.N. Tuama et al., Unveiling the potential of elettaria cardamomum husk ash as feedstock nanofibers in improving the structure, optical, dielectric, and antibacterial performance of peo polymer for optoelectronic and biological applications. Nano Biomed. Eng. (2024). https://doi.org/10.26599/NBE.2024.9290080
34. I.S. Elashmawi, A.M. Ismail, A.M. Abdelghany et al., Electrical investigation and enhancement of optical, structural, and dielectric properties of flexible PVDF/$LiZnVO_4$ nanocomposites. Discov Mater. **3** (2023). https://doi.org/10.1007/s43939-023-00053-7
35. A.M. Salem, A.R. Mohamed, A.Y. Yassin, The effect of low concentrations of polypyrrole on the structural, thermal, and dielectric characteristics of CMC/PPy blends. J. Mater. Sci: Mater. Electron. **34**, 1522 (2023). https://doi.org/10.1007/s10854-023-10938-1
36. A.Y. Yassin, Dielectric spectroscopy characterization of relaxation in composite based on (PVA–PVP) blend for nickel–cadmium batteries. J. Mater. Sci: Mater. Electron. **31**, 19447–19463 (2020). https://doi.org/10.1007/s10854-020-04478-1
37. E. Al-Bermany, A.T. Mekhalif, H.A. Banimuslem et al., Effect of green synthesis bimetallic Ag@SiO2 core–shell nanoparticles on absorption behavior and electrical properties of PVA-PEO nanocomposites for optoelectronic applications. Silicon. (2023). https://doi.org/10.1007/s12633-023-02332-7